# Deformation textures and mechanisms in the granodiorite from the Nojima Hirabayashi borehole

Anne-Marie Boullier[1], Benoît Ildefonse[2], Jean-Pierre Gratier[1], Koichiro Fujimoto[3], Tomoyuki Ohtani[3] and Hisao Ito[4].

*1 - Laboratoire de Géophysique Interne et Tectonophysique, University Joseph Fourier, BP 43, 38041 GRENOBLE cedex, France*
*2 - Laboratoire de Tectonophysique, University of Montpellier II, Place E. Bataillon, 34095 MONTPELLIER cedex 5, France*
*3 - Geological Survey of Japan, Geothermal Department, 1-1-3 Higashi, Tsukuba, Ibaraki 305-8567, Japan*
*4 - Geological Survey of Japan, Earthquake Research Department, 1-1-3 Higashi, Tsukuba, Ibaraki 305-8567, Japan*

## ABSTRACT

The deformation textures in the granodiorite from the Nojima Hirabayashi borehole are described and attributed to aseismic or seismic deformation mechanisms. Aseismic deformation appears to be non negligible even in the low-strain granodiorite (2-5%). It is also present in the cataclasites and ultracataclasites where it alternates which seismic episodes on the fault.

The observed textures throughout the borehole result from the mobility of quartz during the first stage of deformation, and of carbonates during the late ones. The same textures have been described also in the San Gabriel fault (California). This suggests that the textures may be attributed to decreasing temperature conditions and that the hanging wall of the Nojima fault has been uplifted, through time, from 3-5 km depth towards the first km of the crust.

## INTRODUCTION

Twenty-five horizontal thin sections from the core of the Hirabayashi borehole were examined in order to describe the small scale deformation textures related to the active Nojima fault. The objectives of this study were to compare the observed textures with what is known from other active fault systems such as the San Gabriel Fault (California), to interpret the textures in terms of deformation mechanisms and to attribute them, if possible, to the seismic or interseismic stages of the fault activity.

The borehole encountered granodiorite and porphyry dikes. Detailed structural, petrographical, mineralogical and geochemical studies of the borehole have been already achieved (Fujimoto et al., submitted; Ohtani et al., submitted, Tanaka et al., 1999). The present preliminary textural study focusses on granodiorite samples from one minor zone of faulting (around 250 m) and from a few intervals above and below the main shear zone (624 m). Major magmatic minerals of these samples are amphibole, biotite, plagioclase, quartz and K-feldspar. In the following study, the textural classification of fault rocks by Sibson (1977) modified by Snoke and Tullis (1998) has been used.

## DEFORMATION TEXTURES IN LOW-STRAIN ZONES

The granodiorite samples display varying degrees of internal deformation of minerals, fracturation and veining. The veins have not been studied in detail because only horizontal thin sections were available and it was not yet possible to decipher precisely the kinematics of these structures.

### BIOTITE

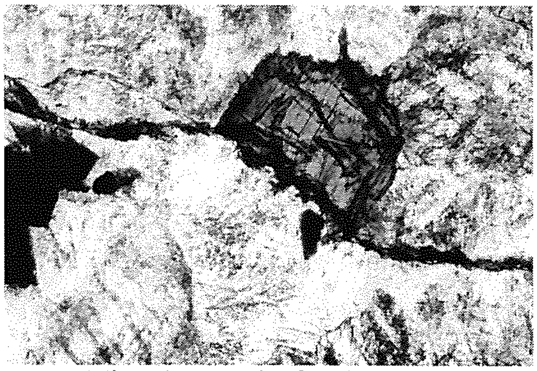

Figure 1. Microphotograph of a kinked biotite in the granodiorite at 352.3 m depth. Note the subhorizontal dark stylolitic plane compatible with the subvertical orientation of the shortened cleavage planes. Thin section is horizontal in the core reference frame. Plane polarized light. The width of the photograph is 3 mm.

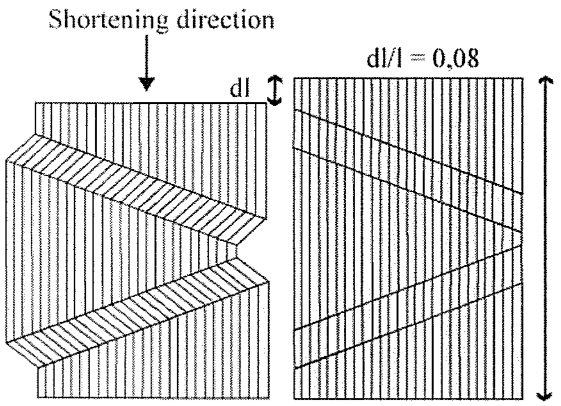


Figure 2. Schematic diagram showing the use of kinked biotites as markers of the shortening direction and of the finite shortening.

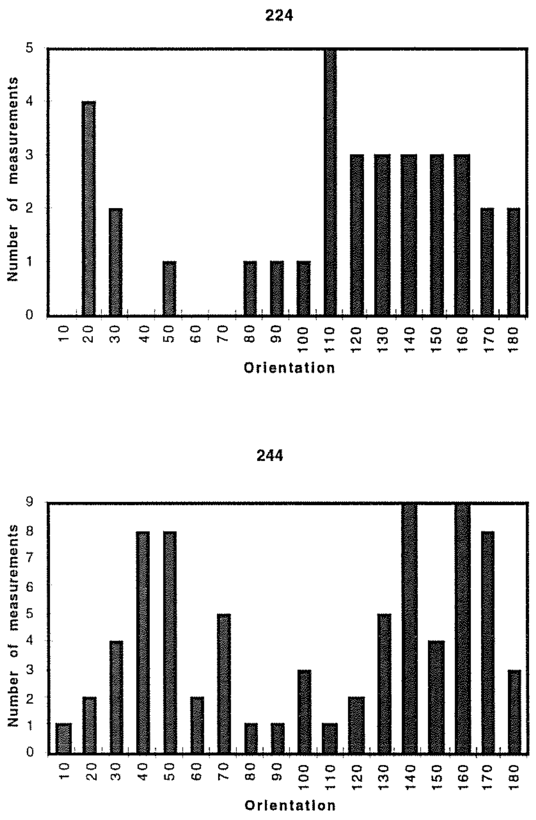


Figure 3. Examples of (001) orientation in kinked biotites for samples at 224.0 and 244.0 m depth. The histograms show two orthogonal directions corresponding to two shortening directions.

Biotite crystals display kink-bands (Figure 1) similar to those described by Kosaka et al. (1999). They indicate, first, the direction of shortening and, second, the finite strain (Figure 2). Generally, and assuming that biotites are randomly orientated throughout the rock, two directions of shortening may be deduced from the orientation of (001) cleavages of the kinked biotite crystals (Figure 3). One direction is more clearly expressed than the other (sharp kink-band boundaries) and in most cases, this direction corresponds, chronologically, to the first one, as established with other structural criteria (veins, microcracks, etc..., see below).

Alteration of biotite may be present, together with kink-bands, and is expressed either by chloritisation along the cleavages or by crystallisation of calcite within the (001) cleavage planes.

The finite shortening of twelve biotites has been determined on one sample (224). Cleavages have been drawn on microphotographs and their length has been calculated using NIH Image program (U.S. National Institute of Health, 1998). The results depend on the location of the crystals: shortening may be as high as 40% for a biotite close to a shear fracture. Generally the shortening is between 2 and 5%.

In some samples, fractures link one biotite crystal to the others, a pattern which suggests that biotites act as soft minerals in the granodiorite.

QUARTZ

Except in the immediate vicinity of the fault, quartz crystals scarcely exhibit classical features of plastic (intracrystalline) deformation such as undulose extinction, subgrains, dynamic recrystallisation (see Kosaka et al., 1999). On the contrary, quartz crystals are intensely fractured and several types of structures may be distinguished:

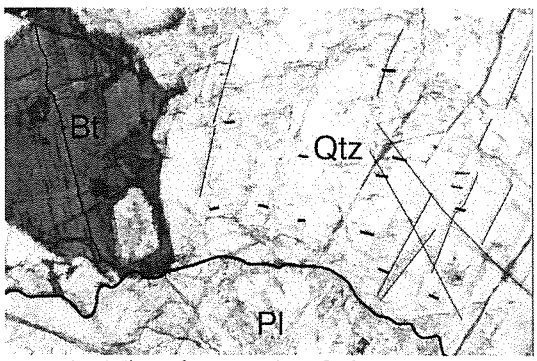


Figure 4. Microphotograph of the 256.2 m core sample (horizontal thin section). The contact between plagioclase (Pl) and quartz (Qtz) has been outlined (thick black line), as well as the shortened (001) cleavage (black line) of biotite (Bt), fluid inclusion planes (thin black line) and flattened fluid inclusions (short thick black lines) in quartz. Fluid inclusion planes and biotite cleavages are radial around the plagioclase boundary which may have acted as a dissolution surface under compressive stress. Plane polarized light. Width of the microphotograph: 3mm.

(i) Fluid inclusion planes are mode I fractures which have been healed by dissolution-crystallisation processes (Tuttle, 1949). The orientation of these fluid inclusion planes is indicative of the stress tensor (Lespinasse and Pêcher, 1986). In the studied samples, the principal orientation of the fluid inclusion planes is coincident with the first direction of shortening deduced from the biotite crystals (Figure 4) and with some small cracks crosscutting plagioclase or K-feldspar and sealed with clear albite or quartz.
(ii) The largest fluid inclusions located within these planes or isolated in the quartz crystals are deformed. They are flattened in short planes or cracks (Figure 4) which have a constant orientation throughout the thin section independantly of the lattice orientation of the quartz crystals.
(iii) Zeolite- or calcite-filled microcracks are present in most of the studied samples, these microcracks have similar orientation to the second shortening direction of (001) biotite cleavages. Generally the zeolite-filled cracks are older than the calcite-filled ones, as already observed by Fujimoto et al. (submitted).

## DEFORMATION TEXTURES IN HIGH-STRAIN ZONES

### CATACLASITES

Four samples of cataclasite (all cohesive) have been observed on horizontal thin sections: one in a minor fault zone at 249.9 m depth, two in the main fault zone at 619.8 and 622.6 m depth, and one, below, at 705.9 m depth. These samples fall into two classes: the silica-cemented (Si-) and the carbonate-cemented (Ca-) cataclasites, depending on the nature of the cementing matrix.
- 249.9 m: a Si-cataclasite is bounded by a sharp shear fracture. In the wall-rock and along this fracture, quartz displays slightly undulose extinction and biotite crystals are highly kinked and smeared out in the shear plane. An undeformed zeolite vein is emplaced along the shear fracture, but no carbonate vein has been observed.
- 619.8 m: quartz is highly fractured and shows only little internal plastic deformation (slight undulose extinction). Biotite is completely altered but the traces of the (001) cleavages are still recognisable and show large shortening (30-40%). K-felspar displays undulose extinction and plagioclase is almost completely replaced (zeolite?). In the preserved fragments of granodiorite, fluid inclusion planes are present and fluid inclusions are flattened perpendicular to these planes. Calcite- and zeolite-filled cracks crosscut the minerals and are approximately parallel to the fluid inclusion planes.

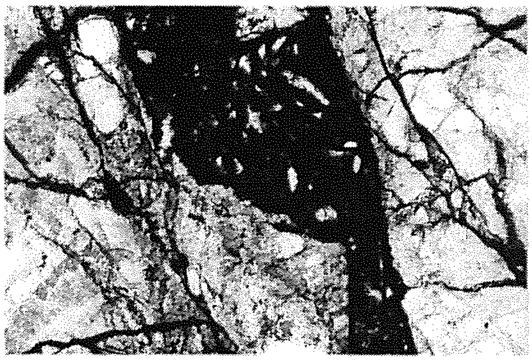

Figure 5. Microphotograph of the 619.8 m depth sample showing the Si-cataclasite (grey) containing some white fragments of quartz, cut by a Ca-cataclasite where small angular fragments of Si-cataclasite are embedded in black siderite cement. Thin section is horizontal in the core reference frame. Plane polarized light. Width of the view: 3 mm.

Twostages are recognized in the cataclastic zones at this level (Figure 5). The first one is a very fine-grained and compacted Si-cataclasite suggesting the activity of dissolution processes. In these Si-cataclasites, impurities and black material are concentrated on irregular stylolite-looking surfaces. Some of these planes are cut by other (younger) cataclastic events and by siderite-filled cracks. The second stage is a Ca-cataclasite with sideritic matrix; it also post-dates the Si-cataclasite

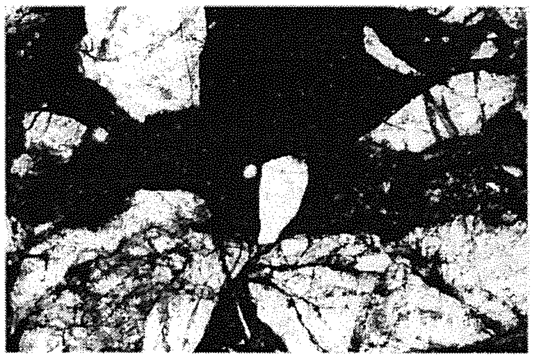

Figure 6. Microphotograph of the 622.6 m depth sample showing grey fragments of Si-cataclasite and quartz embedded in the black cement of the Ca-cataclasite. Thin section is horizontal in the core reference frame. Plane polarized light. Width of the view: 1.5 mm. - 622.6 m: This sample is almost completely cataclastic at the scale of the thin section. Both Si-cataclasites and Ca-cataclasites are observed. Fragments of Si-cataclasites are embedded in younger Si-cataclasites, and Si-cataclasites are themselves fragmented and embedded in Ca-cataclasite with highly variable percentage of carbonate cement. In the cement, euhedral crystals of carbonate may be observed within an unrecognized matrix, at high magnification on the petrographic microscope (see also description of fault gouge at 623.5m by Fujimoto et al., 1999).

Stylolitic planes are visible in the Si-cataclasite and are cut, in some places, by Ca-cataclasites. The latter are also cut by stylolitic planes.

- 705.9 m: this cataclastic sample appears to be more structured than the former ones, although the texture within the wall rock is very similar (highly fractured quartz, flattened fluid inclusions, etc...). The center of the high-strain zone is a foliated and colour-banded Si-cataclasite, displaying some C-S structures similar to those described by Lin (1999) (Figure 7). However, the foliation is defined by a compaction of the very fine-grained angular fragments rather than by internal deformation of them. Colour banding seems to be induced by the alternation of Ca-cataclasites in Si-cataclasites. Again irregular surfaces of dissolution are observed, and compaction appears to be higher in Si-cataclasites than in Ca-cataclasites.

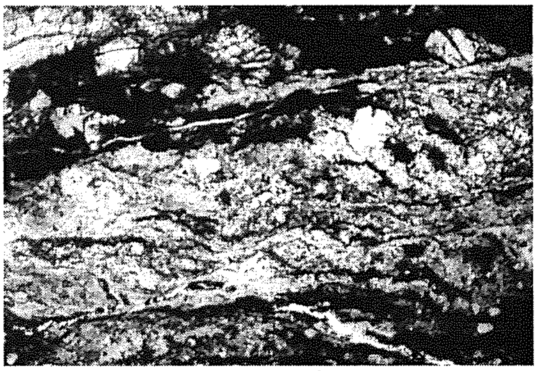

Figure 7. Microphotograph of the 705.9 m depth sample showing the cataclasite with a C (subhorizontal) and S (deeping to the right) structure. Thin section is horizontal in the core reference frame. Plane polarized light. Width of the view: 6 mm.

In summary, it appears that Si-cataclasites are formed first, and are subsequently followed by Ca-cataclasites and siderite-filled cracks. In the cataclasites, episodes of dissolution and veining seem to alternate with episodes of cataclasis.

## DEFORMATION TEXTURES IN THE CORE OF THE MAIN SHEAR ZONE

Two very fragile samples of cohesive fault gouge have been observed at 624.30 and 624.60 m. They are very fine-grained and show a millimetric colour banding suggesting a succession of multiple cataclastic episodes. The banding of the ultracataclasite is cross-cut and displaced along fractures which are filled with zeolites(?) and different layers display varying degrees of fracturation (Figure 8). These samples correspond to the gouge type II as defined by Fujimoto et al. (1999).

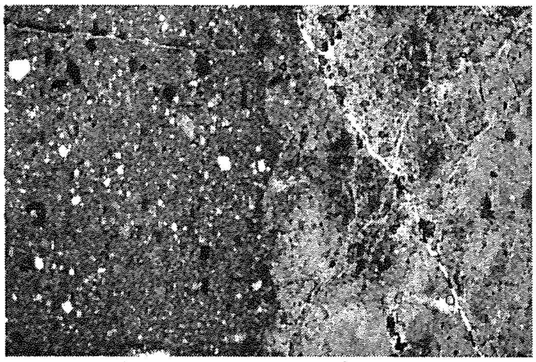

Figure 8. Microphotograph of the 624.6 m depth sample showing the colour banding (vertical). Note that each episode contains fragments of crystals or cataclasite and that the episode on the left is much less fractured than the one on the right. Plane polarized light. Width of the view: 6 mm.

Figure 9. Microphotograph of the 624.6 m depth sample showing the colour banding (horizontal) and some stretched folded fragments within the central episode. Plane polarized light. Width of the view: 6 mm

Within the colour banding, it is possible to recognise elements of older ultracataclasite embedded in younger ultracataclasite. The fragments sometimes display folding suggesting structures described in pseudotachylites (Figure 9). The isotropic character (black under polarised and analysed light) of the very fine matrix in some of the bands, reinforce the similarity with pseudotachylite. However, this isotropic character may be due to very fine grain-size of the matrix and no absolute evidence has been found for the presence of glass under the petrographic microscope. Further detailed studies (SEM, TEM) are necessary to test the presence or absence of a molten phase.

## COMPARAISON WITH TEXTURES IN THE SAN GABRIEL FAULT

In Southern California, recent uplifting of the San Gabriel mountains (along thrust faults) exposed crustal levels from about 2 to 5 km depth (Oakeshott, 1971).

Microstructures and mineral assemblages of the outcropping fault rocks are consistent with right lateral strike-slip faulting at depth (Jennings, 1994).

Samples were collected in granites several meters to hundreds of meters away from the central gouge zone. The crack orientation indicates the direction of shortening, and ranges from 020° to 045° with respect to the faults. This variation may be related to successive seismic events with associated crack sealing processes. Quartz is the most frequent mineral filling the sealed cracks. However, a network of very thin veins, filled with calcite, is seen by cathodoluminescence studies and is the latest episode of crack sealing.

Dissolution features can be distinguished in the samples. The sealed cracks (T) are associated with, and are perpendicular to, solution cleavage (S in Figure 10a). Most of the veins are interrupted against solution cleavage, this relation indicating their closed relationship (Figure 10). This solution cleavage can be seen at the scale of several grains or at the scale of a single grain boundary.

A schematic restored state, before solution along stylolites, (Figure 10b) shows the location of the transgranular zone of dissolution, and the associated veins which are interrupted against the zone of dissolution. Quartz and feldspar both show evidence for dissolution under stress. The aperture of the cracks (or at least the thickness of the filling material) may be estimate when the sealing mineral is different from the host mineral (for example quartz veins in feldspars); it ranges from 10 to 100 µm. Apertures are more difficult to estimate when the sealing and the host mineral are not easily differentiated. Example of transgranular cracks in quartz shows that the two limits of the cracks are often outlined by two trails of fluid inclusions in the host mineral.

Other samples were collected from various sites in Southern California (Gratier et al., 1994) allowing the observation of pressure solution and crack sealing in rocks brought up from several kilometers depth (from 1-2 to 5-10 km). Mass change and mobile elements associated with pressure solution-deposition have been estimated by comparative chemical analysis. The relative mobility of quartz and calcite clearly evolves with depth. At low depth, calcite is more mobile than quartz, and this relative mobility reverses at larger depth. This is consistent with the theoretical evolution of pressure solution strain-rate with depth for these two mineral (Gratier, 1984, Figure 11). This evolution is related to two converging effects:

- the solubilities of quartz and calcite show an inverse evolution with increasing temperature (normal and reverse relation, respectively, for quartz and calcite),
- at low temperature the kinetics of quartz dissolution is very low and prevents significant pressure solution process (Oelkers et al., 1996; Renard et al., 1997).

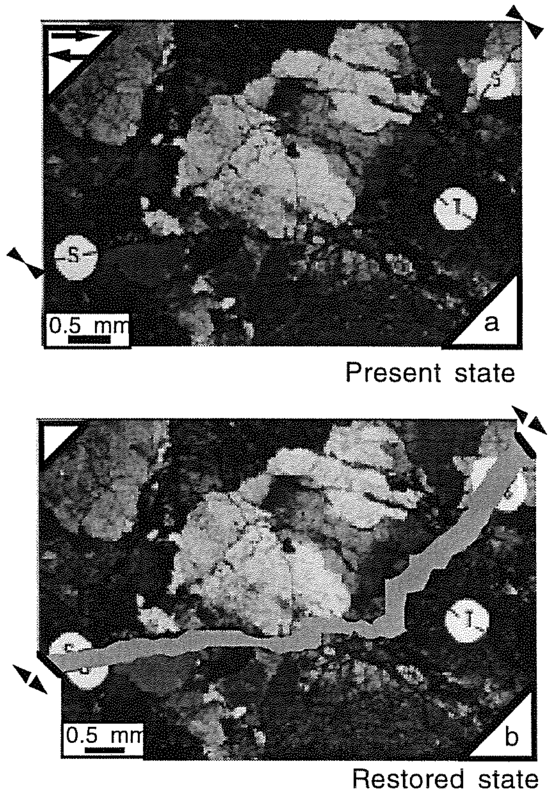


Figure 10. Microphotograph of an horizontal thin section from a granitic rock of the San Gabriel fault (Gratier et al., 1994). (a) present state: S is the stylolitic plane and T is a sealed crack. (b) restored state showing the dissolved mater along the stylolitic plane. Plane polarized and analysed light.

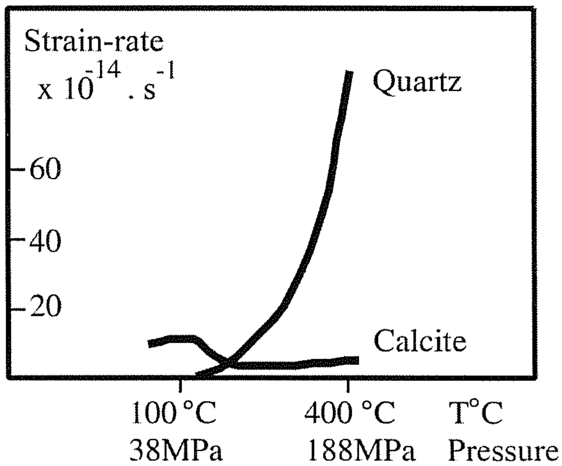


Figure 11. Theoretical diagram showing the strain-rate versus the P and T conditions for quartz or calcite aggregates (after Gratier, 1984).

## DISCUSSION

Several important facts must be pointed out. First, it is possible to recognize some deformation textures in the low-strain granodiorite, which indicate a succession of two-shortening directions (two stress tensors), each one corresponding to a few percent of strain (2-5%).

The first stage corresponds to temperature conditions in which silica is mobile since mode I cracks are healed (fluid inclusion planes) and fluid inclusions are flattened due to dissolution-crystallisation processes in quartz (Tuttle, 1949; Gratier and Jenatton, 1984). Microthermometric measurements on fluid inclusions in quartz from granodiorite core samples indicate relatively high homogenisation temperatures (ca 300°C, Ohtani et al. Submitted). The authors interpret these fluid inclusions as representing fluids trapped during cooling of the granodiorite. Moreover, the 3-D orientation of the fluid inclusion planes is not compatible with the present-day state of stress accompanying a reverse dextral sense of shear on the Nojima fault as demonstrated by Takeshita and Yagi (1999). Therefore, and following these authors, the fluid inclusion planes may represent Late Cretaceous microcracks healed at temperature above 300°C immediately after the solidification of the granodiorite in a tectonic setting corresponding to left-lateral movement on a "proto-Nojima" fault (Takeshita and Yagi, 1999).

The second event corresponds mostly to calcite-filled cracks and, therefore, to temperature conditions in which calcite is mobile. Since the two filling minerals (quartz and calcite) have opposite behaviours, we may deduced that the observed textures correspond to decreasing temperature conditions: above ca 180°C for quartz, and below that temperature for calcite (Gratier, 1984; Figure 11). A low temperature (ca 50°C) is also suggested for alteration and calcite deposition in cracks and veins by Ueda et al. (1999), on the basis of stable isotope data. These textures involve slow processes (dissolution, diffusion and crystallisation, Gratier & Gamond 1990) and therefore are assumed to be aseismic.

The second important point is that the same succession of mobile minerals may be observed in cataclasites, except in the 249.9 m sample, where no carbonate veins or cracks have been observed. In this zone, only Si-cataclasites are present. This suggests that this cataclastic zone has been active only at temperatures higher than ca 180°C and, therefore, that it is a to-day inactive and uplifted small fault zone. In the main shear zone, Ca-cataclasites post-date the Si-cataclasite, indicating that it has been uplifted through time, which is consistent with the reverse oblique movement on the Nojima fault.

The third important point is that, in all cataclasites and ultracataclasites, it was possible to observe dissolution structures or mineralised fractures alternating with cataclastic episodes and mutual cross-cutting relations. This suggests that slow strain-rate (aseismic) processes such as dissolution-crystallisation alternate with high strain-rate (seismic) processes such as cataclasis and friction.

Finally, it was not yet possible to determine if melting occurred due to friction within the main shear zone. However, the flow structures (folds) suggest an intermediate viscous behaviour between a molten material (pseudotachylite) and a very finely crushed one (ultracataclasite) in the fault core.

## CONCLUSION

The deformation textures in the granodiorites from the Nojima Hirabayashi borehole are ascribed to aseismic or seismic deformation mechanisms (Gratier and Gamond, 1990; Gratier et al., 1999).

Aseismic deformation due to dissolution-crystallisation processes appears to be significant even in the low-strain granodiorite (2-5%). It is present also in the cataclasites and ultracataclasites where it alternates which seismic episodes on the fault. The observed textures result from the mobility of quartz during the first stages and of calcite during the late ones, which suggests that they may be attributed to decreasing temperature conditions and that the hanging wall of the fault has been uplifted through time, from 3-5 km depth towards the first kilometer of the crust.

The dissolution-crystallisation processes observed during aseismic intervals allow a modification of the permeability of rocks and, therefore, a variation in fluid pressure (Blanpied et al., 1992; Rice, 1992; Gratier et al. 1994). The fluctuations in fluid pressure may, in turn, enhance the seismic rupture on the high-angle reverse Nojima fault (Sibson et al., 1988).

## ACKNOWLEDGEMENTS

This study would not have been possible without the excellent thin sections realised on difficult material and in hurry by Christophe Nevado at the Montpellier University. This work is funding by GdR FORPRO (action 99.V, publication FORPRO 99/005 B).

## REFERENCES

Blanpied, M., Lockner, D. and Byerlee, J. 1992. An earthquake mechanism based on rapid sealing of faults. *Nature* **358**, 574-576.

Chester, F. M., Evans, J. P. and Biegel, R. L. 1993. Internal structure and weakening mechanisms of the San Andreas fault. *Journal of Geophysical Research* **98**, 771-786.

Fujimoto, K., Tanaka, H., Tomida, N., Ohtani, T. and Ito, H. 1999. Characterization of fault gouge from GSJ Hirabayashi core samples and implications for the activity of the Nojima fault. In: *International workshop on the Nojima fault core and borehole data analysis*, Tsukuba, Japan. Extended abstracts.

Fujimoto, K., Tanaka, H., Higuchi, T., Tomida, N., Ohtani, T. and Ito, H. submitted. Alteration and mass transfer along the GSJ Hirabayashi borehole penetating the Nojima earthquake fault, Japan. *Island Arc*.

Gratier, J. P. 1984. La déformation des roches par dissolution-cristallisation: aspects naturels et expérimentaux de ce fluage avec transfert de matière dans la croûte supérieure. Unpublished Thèse d'Etat thesis, Université Joseph Fourier.

Gratier, J. P., Chen, T. and Hellman, R. 1994. Pressure solution as a mechanism for crack sealing around faults. In: *Proceedings of Workshop LXIII: The Mechanical Involvement of Fluids in Faulting* **Open-File Report 94-228**. U.S. Geological Survey, 279-300.

Gratier, J. P. and Gamond, J. F. 1990. Transition between seismic and aseismic deformation in the upper crust. In: *Deformation mechanisms, rheology and tectonics* (edited by Knipe, R. J. & Rutter, E. H.) **54**. Geological Society Special Publication, 461-473.

Gratier, J. P. and Jenatton, L. 1984. Deformation by solution - deposition and reequilibration of fluid inclusions in crystals depending on temperature, internal pressure and stress. *Journal of Structural Geology* **5**, 329-339.

Gratier, J. P., Renard, F. and Labaume, P. 1999. How pressure-solution and fractures interact in the upper crust to make it behave in both a brittle and viscous manner. *Journal of Structural Geology* **21**, 1189-1197.

Jennings, C. W. 1994. Fault activity map of California and adjacent areas with location and ages of recent volcanic eruptions. California Division of Mines and Geology.

Kosaka, K., Shimizu, M. and Takizawa, S. 1999. Delineation of deformation grades of low-strain granitoids using assemblages of elementary deformation textures. *Journal of Structural Geology* **21**, 1525-1534.

Lespinasse, M. and Pêcher, A. 1986. Microfracturing and regional stress field : a study of the preferred orientations of fluid-inclusion planes in a granite from the Massif Central, France. *Journal of Structural Geology* **8**(2), 169-180.

Lin, A. 1999. S-C cataclasite in granitic rock. *Tectonophysics* **304**, 257-273.

Oakeshott, G. B. 1958. Geology and mineral deposits of San Fernando quadrangle. *California Division of Mines and Geology Bulletin* **172**, 147pp.

Oakeshott, G. B. 1971. Geology of the epicentral area. *California Division of Mines and Geology Bulletin* **196**, 19-30.

Oelkers, E. H., Bjørkum, P. A. and Murphy, W. M. 1996. A petrographic and computational investigation of quartz cementation and porosity reduction in North Sea sandstones. *American Journal of Science* **296**, 420-452.

Ohtani, T., Tanaka, H., Fujimoto, K., Higuchi, T., Tomida, N. and Ito, H. submitted. Internal structure of the Nojima fault revealed by the GSJ borehole. *Island Arc*.

Renard, F., Ortoleva, P. and Gratier, J. 1997. Pressure solution in sandstones: Influence of clays and dependence on temperature and stress. *Tectonophysics* **280**, 257-266.

Rice, J. R. 1992. Fault stress states, pore pressure distributions, and the weakness of the San Andreas Fault. In: *Fault mechanics and transport properties in rocks* (edited by Evans, B. & Wong, T. F.). Academic Press, 475-503.

Sibson, R. H. 1977. Fault rocks and fault mechanisms. *Journal of the Geological Society of London* **133**, 191-213.

Sibson, R. H., Robert, F. and Poulsen, K. H. 1988. High angle reverse fault, fluid-pressure cycling and mesothermal gold quartz deposits. *Geology* **16**, 551-555.

Snoke, A. W. and Tullis, J. 1998. An overview of fault rocks. In: *Fault-related rocks: a photographic atlas* (edited by Snoke, A. W., Tullis, J. & Todd, V. R.). Princeton University Press, Princeton, New Jersey, 3-18.Takeshita, T. and Yagi, K. 1999. Dynamic analysis based on 3-D orientation distribution of microcracks in quartz from the Cretaceous granodiorite core samples deilled along the Nojima fault, southwest Japan. In: *International workshop on the Nojima fault core and borehole data analysis*, Tsukuba, Japan. Extended abstracts.

Tanaka, H., Tomida, N., Sekiya, N., Tsukiyama, Y., Fujimoto, K., Ohtani, T. and Ito, H. 1999. Distribution, deformation and alteration of fault rocks along the GSJ core penetrating the Nojima fault, Awaji Island, Southwest Japan. In: *International workshop on the Nojima fault core and borehole data analysis*, Tsukuba, Japan. Extended abstracts.

Tuttle, O. F. 1949. Structural petrology of planes of liquid inclusions. *Journal of Geology* **57**, 331-356.

Ueda, A., Kawabata, A., Fujimoto, K., Tanaka, H., Tomida, N., Ohtani, T. and Ito, H. 1999. Isotopic study of carbonates in Nojima fault cores. In: *International workshop on the Nojima fault core and borehole data analysis*, Tsukuba, Japan. Extended abstracts.